

GUIDED IMPACT FUSION

v1.1

ColinBJ@gmail.com

© Colin Jack 2009-2012

CONTENTS

ABSTRACT	2
1. BASELINE DESIGN	3
2. DEVELOPMENT AND OPTMIZATION	25
APPENDIX : force calculations	28
REFERENCES	30

ABSTRACT

There is a practical way to generate energy from fusion. The basic method is well known: a hollow fuel capsule implodes within a hohlraum. However the hohlraum is heated not by lasers, but by the impact of charged micropellets fired at ultravelocity. This technique has long been used to test spacecraft micrometeoroid shields, and has been suggested for fusion. The key novel step is that it is now possible to track and guide each pellet individually during flight, using COTS-available technology. This opens up options never before considered:

- The pellets catch up together during flight through a long vacuum pipe, so an accelerator of modest power can provide a very high peak input pulse. A train of pellets launched over a period of milliseconds arrives at the hohlraum within a span of nanoseconds: a 'temporal compression' factor of one million.
- Successively smaller course corrections fine-tune the pellet trajectories to ever-increasing precision. The pellets are progressively discharged as they travel, so mutual repulsion at convergence is eliminated. The pellets impact the hohlraum in a precisely specified pattern.

The method is ideally suited to standoff operation. Detonation can take place completely surrounded by flowing lithium, which extracts the energy while also breeding tritium to close the fuel cycle. There is no need for a large vacuum chamber, and no unwanted radioactives are produced.

The only net input is deuterium and lithium. Capital cost is modest. Equipment life is indefinite. It will be possible to retrofit existing coal-fired generating plant for fusion.

Overall length of the accelerator and standoff pipe is substantial, several kilometres. However even if the whole length has to be placed in a tunnel, its cost is small compared to that of a power station. The pellets travel at only a few hundred km/sec: the accelerator is driven at RF frequency, by inexpensive solid state switches.

1. BASELINE DESIGN

To minimize technical uncertainty and facilitate comparison, the Baseline Design uses a hollow spherical fuel capsule identical to those developed for laser driven fusion, and driven by an identical X-ray pulse generated within a hohlraum. The capsule contains deuterium-tritium fuel. The X-rays evaporate material from its outer wall, causing it to implode by reactive force, compressing and igniting the fuel.

2.1 HOHLRAUM ACTION

In light of the National Ignition Facility's performance problems, a larger fuel capsule is assumed, as designed for NIF's intended successor LIFE. Moreover an increase in capsule absorbed energy from LIFE's baseline value of 0.77 MJ to 1.0 MJ is assumed. Design parameters for NIF, LIFE and Guided Impact Fusion GIF are compared in Table 1.

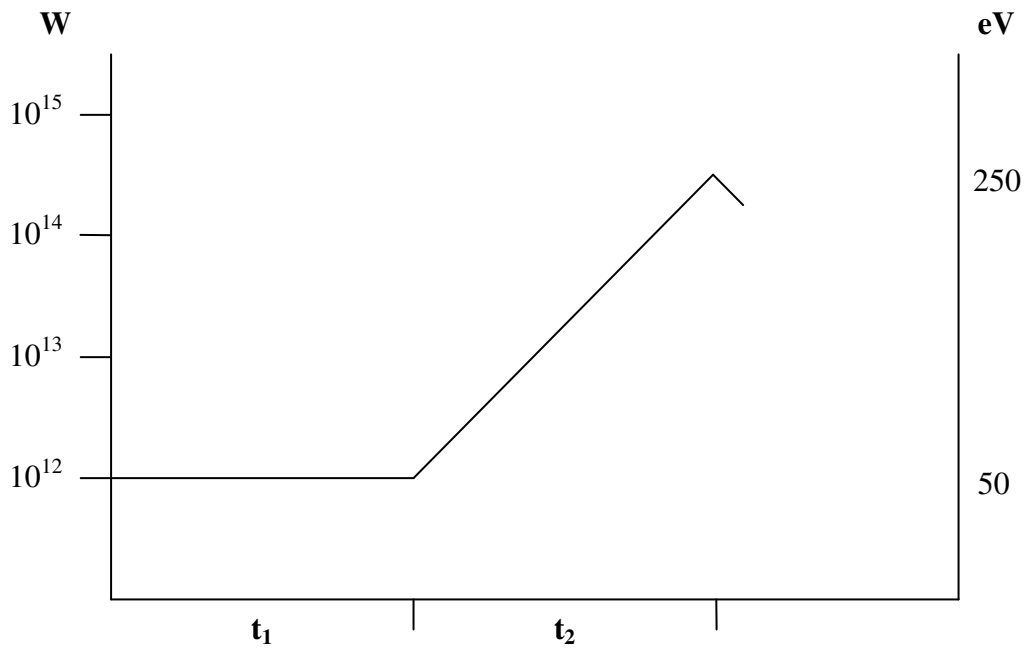
Note that for GIF, the conservative assumption is made that just 12.5% of the energy entering the hohlraum reaches the capsule as X-rays. This is in contrast to the highly optimistic 25-35% projected for NIF and LIFE. Because electric acceleration of pellets is far more efficient than electric generation of laser energy (70-90% whereas even future generation lasers of suitable type^[3] are unlikely to do better than 18%) GIF nevertheless achieves a more favourable output ratio.

TABLE 1

		NIF	LIFE ^[1]	GIF
capsule diameter	mm	2.2	4.1	4.1
hohlraum max temperature	eV	300	250	250
energy delivered to hohlraum	MJ	1.8	2.2	8.0
energy delivered to capsule	MJ	0.2-0.45	0.77	1.0
fusion thermal output	MJ	16	200	200

The shape of the X-ray input pulse required is shown in Figure 1: an initial period t_1 of constant energy rate, which then rises exponentially over a period t_2 to peak at ~ 500 times the initial value. This is equivalent to black-body radiation temperature rising from 50 to 250 eV.

FIGURE 1 Pulse variation with time^[adapted from 2, p50]



W power received by capsule, watts

eV temperature, (1 eV \sim 11,600 degrees Kelvin)

t1, t2 \sim 20 nanoseconds each: power doubles every \sim 2 ns during rise

The GIF hohlraum is shown in Figure 3, beneath the LIFE hohlraum drawn at the same scale in Figure 2 for comparison. The GIF hohlraum is asymmetric because pellets approach from one direction only (the left).

FIGURE 2 LIFE hohlraum (major features to scale)

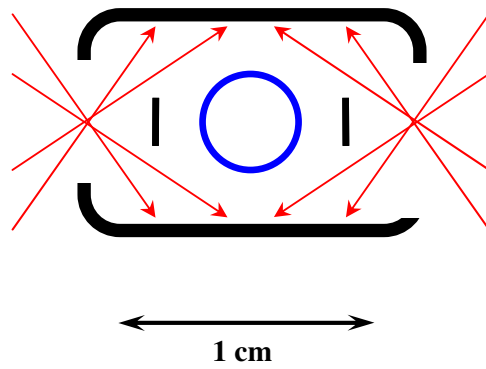
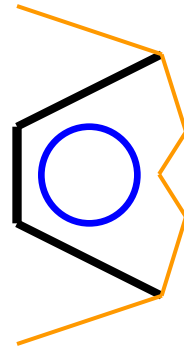


FIGURE 3 GIF hohlraum (major features to scale)

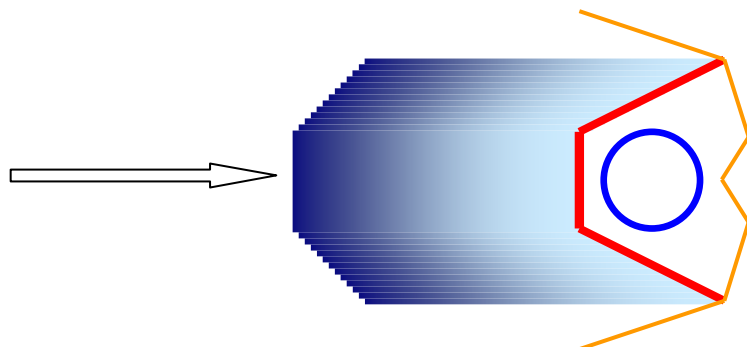
a Initial



b Leading pellets hit foil heating it to 50eV; main pellet cloud approaches



c Main pellet cloud arrives



To release their energy, the incoming pellets need to strike a stationary mass: this is provided as the membrane shown in black in Figure 3a.

A first wave of pellets, comprising $\sim 3\%$ of the total pellet mass, strikes this membrane, heating it by shockwave to form a 'collision plasma' at 50eV as shown in Figure 3b. 20 nanoseconds later the main pellet cloud arrives as shown in Figure 3c.

The internal density distribution of the main pellet cloud is chosen such that the collision plasma temperature then increases exponentially over a further 20 ns period. The internal velocity distribution and density of the pellet cloud can be set with exquisite precision in software alone and fine-tuned empirically: in a first approximation, pellets further from the axis travel faster as illustrated, so that the right hemisphere of the fuel capsule is heated as strongly as the left, despite receiving most of its energy indirectly via the hohlraum.

A suitable pellet speed is ~ 700 km/sec, so each pellet moves about 0.7 mm per nanosecond. The pellet speeds actually range from 630 to 770 km/sec. Total pellet kinetic energy is 8 MJ, total pellet mass is 33 mg.

Throughout the process, the collision plasma moves forward relative to the original membrane position due to conservation of momentum. Almost all of this movement results from first wave impact, as while the second wave is bigger, most of its mass arrives only in the final nanoseconds. Total movement over the 40-nanosecond period is ~ 0.3 mm. By this point, the fuel capsule surface is already imploding at a rate greater than the collision plasma is approaching. There is no need for large clearance between the membrane and the fuel capsule because (a) the pellets can be distributed in a precise pattern to heat the membrane very evenly, unlike the case with a laser pulse heating a hohlraum wall; (b) the rocket-exhaust evaporation from the surface of the fuel capsule itself protects it from interaction with the collision plasma.

The fuel capsule experiences a temperature environment, an X-ray 'bath', identical to that planned for laser-driven fusion. The capsule implodes and ignites under its own momentum.

In order to make the energy transfer from the collision plasma to the fuel capsule as efficient as possible, the following considerations should be respected.

- The pellet cloud should collide with a fixed membrane of greater mass than itself, so that not too much energy is wasted as linear motion of the collision plasma. A membrane mass of twice the total pellet mass is assumed, making this loss 33%.
- The remaining energy should be enough to heat the collision plasma (if all heat were retained in the plasma) to a temperature several times higher than actually required. Heat is usefully radiated until the collision plasma temperature falls about 10% below the peak value needed, to ~ 225 eV. Thermal energy sufficient to heat the plasma to ~ 800 eV (if none escaped during the process) is provided, so 28% of this heat energy is wasted, retained in the collision plasma at the end of the process.
- The specific heat capacity of the collision plasma should not be too high. Equipartition of energy causes the kinetic energy present to be distributed equally between all independently moving particles present, each nucleus and electron carrying an equal amount. (The plasma density is not high enough for Fermi degeneracy to reduce the energy taken up by the electrons.) To minimize specific heat capacity, average particle mass should be maximized, so nuclei incorporating neutrons are desirable, i.e. anything heavier than ordinary hydrogen. Average particle mass will then be ~ 2 a.u.

To radiate the maximum amount of heat forward towards the capsule, the collision plasma should not be of uniform atomic composition: the average atomic mass should be low at the forward side of the plasma, high at the rearward side. This ensures that:

- More collision shock energy is dissipated in the forward part of the collision plasma, nearest the fuel capsule, relative to the rearward.
- Heat can flow more easily toward and out of the forward side of the collision plasma than the rearward, because material of lower z -number is more transparent to X-rays.

The membrane should therefore have a lower average atomic mass than the pellets. The pellets must have high tensile strength to carry the highest possible charge/mass ratio without bursting apart: as explained below, plausible choices include aluminium-lithium alloy microspheres, maraging steel microspheres, or a strong allotrope of carbon such as diamond. The X-ray opacity of plasma from these materials at the lowest and highest operational plasma temperature is shown in Table 2.

TABLE 2 Rosseland opacity of plasma (cm²/g) [4][2,p359]

Material	Main elements	Opacity @ 50 eV	Opacity @ 250 eV
Diamond	Carbon 100% (z=6)	1000	10
Weldalite 049	Aluminium 92% (z=13) Copper 6% (z=29) Lithium 1.3% (z=3)	8000	20
Maraging steel	Iron 70% (z=26) Nickel 18% (z=28) Cobalt 8% (z=27)	12000	200

The membrane area is ~1 cm², its initial mass 0.66 g. The total pellet mass is 0.33g. Total collision plasma areal density rises from 0.7 g/cm² to 1.0 g/cm² during the process. Radiant energy need escape only relatively gradually during the preheat phase at 50 eV, which lasts 20 ns, but must escape rapidly, within ~1 ns, at the peak 250 eV.

A good choice of materials is therefore: carbon for the membrane, aluminium-lithium alloy for the majority of pellets, maraging steel for the final 10% of the pellets.

On collision the following sequence of events occurs:

- A first wave of about 3% of the total pellet mass strikes the membrane, producing plasma at 50 eV moving forward at 7 km/sec = 7 $\mu\text{m/ns}$.
- Over the next 20 ns another 1% of the pellet mass reaches the collision plasma, maintaining its temperature at 50 eV as energy is radiated at a constant rate.
- For the next 20 ns pellet mass strikes the collision plasma at an exponentially increasing rate, raising its temperature to a peak 250 eV as it simultaneously radiates energy.

After the first wave strikes, energy radiated to rearward ensures that subsequent pellets reach the collision plasma already preheated from solid to plasma. Most of the rearward radiated energy is therefore not lost but returned to the collision plasma by the forward movement of the oncoming pellet mass. In the final stages, the high-z plasma from the final 10% of pellets made from maraging steel acts as a 'cap' to reduce the rearward escape even of the highest temperature 250 eV radiation.

Overall efficiency of the process is estimated as follows.

- The pellets have total kinetic energy 8 MJ. Of this one-third is wasted as linear motion of collision plasma.
- The remaining 5.3 MJ would heat the collision plasma to 800 eV if none were radiated. At its final temperature of 225 eV the collision plasma retains 28% of this, 1.5 MJ, so 3.8 MJ is radiated as X-rays.
- Over half this, conservatively put at 2 MJ, is radiated forward. The right and left halves of the fuel capsule should be considered separately. The left hemisphere receives essentially all its radiation directly from the closely adjacent collision plasma: 0.5 MJ. The right hemisphere receives radiation mainly indirectly, via the hohlraum wall. Hohlraum wall losses are approximately two-thirds, so this hemisphere should be sent 1.5 MJ to receive 0.5 MJ.

A total of 1 MJ is thus supplied to the fuel capsule, as required.

2.2 PELLETS

Charged pellets can be accelerated to extreme speeds in a modified particle accelerator, a technique used since the 1960s to simulate the effect of ultravelocity micrometeoroid impacts on spacecraft. A landmark Los Alamos design^[5] included chicane-style wiggles to exclude all material not of the correct mass and charge, so that the accelerator remained clean of conducting dust and performed perfectly in continuous operation, even when the pellet source was a very imperfect monodisperse: commercially available iron microspheres of variable size contaminated with nanoparticles.

To minimize accelerator length, pellet charge/mass ratio should be maximized. The pellets should be given positive rather than negative initial charge, to avoid field effect electron current leakage, and to permit later controlled charge reduction by electron addition. The maximum charge which can be placed on them is limited by two closely related effects: field effect evaporation of atoms from the surface, and burst-apart due to mutual charge repulsion. At ordinary temperatures burst-apart is the limiting factor.

The additional stress due to applied acceleration $\sim 10^7 g$ is small compared to self-repulsion. However, as they proceed through a 2-phase accelerator, the pellets experience force cycling rapidly from maximum between electrodes to zero within an electrode. This does no harm to an electron or atomic nucleus, but repeatedly flexes a larger object, and induces an alternating voltage across it. The pellets must therefore satisfy the following criteria:

1. High specific strength, for high charge/weight ratio
2. High stiffness, so do not melt due to flexural heating
3. Must not be damaged by induced voltage or current
4. Must be reasonable cost

Achievable charge/mass ratio, as calculated in the Appendix, is:

$$Q/M = \frac{1.26 \times 10^{-5} \sqrt{\sigma}}{R\rho}$$

where **R** is the radius, **ρ** the density and **σ** the permissible tensile stress.

To satisfy criterion 2, the stiffness/density ratio should be sufficient that the propagation time of a compression/tension wave across the pellet is less than the accelerator cycle time at the maximum frequency used.

To satisfy criterion 3, the pellet should either be conducting so that surface charge can flow freely, or else have dielectric strength greater than the peak accelerator voltage gradient experienced.

Physically appropriate choices are shown in Table 3.

TABLE 3 Pellet candidate materials

material	density	strength GPa	relative accelerator length
Diamond UNCD	3.5	3.0 ^[6]	1
Maraging steel	8.1	2.4 <i>yield</i>	2.2
Al-Li Weldalite 049-T8	2.7	0.69 <i>yield</i> ^[7]	2.4

Diamond would be ideal. However it is too expensive. About 30 kg/day of pellets will be required for a 1 GW power station. While sieved diamond powder is available at cost ~\$5/g, synthetic diamond of strength comparable to natural diamond and capable of being cut into pellets of precise shape and size would be UNCD (ultra-nano-crystalline diamond) which currently costs ~\$10,000/g; even ordinary CVD diamond coating, which is already produced in quantity but far less strong, costs ~\$500/g.

By contrast metal alloys cost only a few dollars per kilogram. Microspheres can be made simply by spraying droplets of molten metal which solidify as they fall, the technique originally used to make ball bearings. Piezoelectrically controlled nozzles for spraying droplets of precise size at a rapid rate are standard technology, used for example in computer printers.

Aluminium-lithium alloy is therefore chosen for the majority of the pellets. The Weldalite™ grade shown reaches its maximum strength without working, by heat treatment alone (hence the trade name) so is ideally suited to making strong microspheres.

Pellet properties are summarised in Table 4. A total of 360,000 pellets are needed per pulse.

TABLE 4 Pellet properties

Material	Al-Li Weldalite 049-T8
Density	2.7 g/cc
Yield strength	0.69 GPa
Diameter	40 μm
Capacitance	2.2×10^{-15} F
Mass	90 ng
Kinetic energy (average)	22 J
Charge	440 pC
Charge/mass ratio	4.9 C/kg
Stress	0.46 GPa (=> safety factor 1.5)
Potential	200 kV
Surface field	1.0* V/Å

*This is comfortably below the level, 2-4 V/Å, at which field effect evaporation from an aluminium surface becomes significant.^[8]

Maraging steel also reaches its maximum strength without working, and is used for the last 10% of the pellets in each input pulse, for which a higher z-number is preferable. It is fortuitous that, as shown in Table 3, achievable charge/mass ratio is very similar for Weldalite and maraging steel, so no problem arises using the same accelerator for both.

2.3 ACCELERATOR

To strike the hohlraum together, pellet launch speeds must vary from 630 to 770 km/sec from start to end of the burst fired. The higher speed corresponds to acceleration through 61 GV potential difference.

In some ways the accelerator resembles a fundamental particle accelerator. However the pellet speed is $\ll 1\%$ lightspeed, so the electrodes do not act as RF resonant cavities: the tube walls should be insulating material rather than metal. Of current designs, the accelerator most closely resembles the 'dielectric wall' under development at Lawrence Livermore^[9] to fire relatively low energy nuclei for medical applications.

The volts per metre achievable are limited by:

- Vacuum breakdown field of electrodes
- Bulk dielectric breakdown strength of insulator
- Surface effect breakdown strength of insulator

Treated electrodes can withstand surface field strengths in vacuo^[10]:

Copper	134 MV/m
Molybdenum	266 MV/m
Tungsten	406 MV/m

Bulk insulating materials such as Teflon and Rexolite are vulnerable to surface flashover, even in vacuo, at field strengths of a few MV/m. However research for the dielectric wall accelerator has shown that insulator suitably interspersed with conducting material, for example a sandwich structure with dielectric layers alternating with thin layers of conductor, or bulk dielectric with metal inclusions, performs much better, to >100 MV/m without either internal breakdown or surface flashover.^[9] This applies even with metal layers or inclusions whose voltage 'floats', unconnected to any external source.

Peak inter-electrode gradient can therefore be at least 100 MV/m. Allowing a safety factor of 1.5, and taking into account that a pellet passing along the tube experiences an average field ~ 0.6 of the peak field

strength, 40 MV/m working value is achievable, giving accelerator length 1.53 km.

An appropriate drive frequency at the relatively low pellet speed (1/400 lightspeed) is 100-200 MHz. Exotic high-frequency sources such as klystrons are not required: at this frequency solid state components work well and are cheaper. An example of a suitable RF power MOSFET is the IXYS IXZ2210N50L^[11], capable of 550W CW output at 175 MHz, whose cost in bulk is ~\$50/unit^[12]. When used to provide power in pulses of length ~1-10 ms, it can deliver ~18 J per pulse, irrespective of the exact pulse length (^[11], IXZ210N50L Safe Operating Area graph, multiplied by 1.8 for model 2210 relative to 210). Thus RF MOSFET cost is ~ \$3 / J pulse.

To make good use of the civil engineering infrastructure, the building should house several accelerator tubes, including a spare to allow continued operation in the event of tube failure. A reasonable choice is 4 operational tubes plus one spare. So 90,000 pellets will be launched from each tube, on beamlines that gradually converge as they travel toward the target.

In each tube, drive frequency is increased uniformly from 126 to 154 MHz between the time the first and last pellets leave the tube. Pellets emerge 5 mm apart: electrode interval is 2.5 mm at the fast end, with voltage cycling between +/-83 kV. To achieve this, the output from the MOSFETs is fed into compact open-core transformers. Allowing for 20% losses downstream of the MOSFETs, total energy 10 MJ must be provided at high frequency, so total MOSFET cost will be **\$30 million** irrespective of other design choices, number of tubes used, etc.

At the low-speed end of each tube there will be a minimum acceptable pellet separation of about 0.5 mm, due to inter-pellet repulsion (as calculated in the Appendix) and practical fabrication constraints. In place of what would be the first 15m of the tube, a low-power leader section ~100m long is therefore provided, with fixed electrode separation 0.25 mm and highly variable drive frequency from 1 MHz to 126 MHz. This section is fed with pellets which are precharged to 5 kV and fired in at 500

m/s from a source at 1 MV potential over a period of 0.09 seconds. The 1 MHz pellet feed rate required is far lower than the rate at which a modern inkjet printer head ejects droplets.

After 0.09 seconds the leader contains 90,000 pellets in a 45m length line, levitated by a DC vertical field component. The variable frequency electrodes then accelerate this line en bloc to 63 km/sec as the front pellets enter the main accelerator at 126 MHz, still at 0.5 mm separation as required. During this process the pellet voltage is raised to 200 kV by offsetting the local electrode voltages to this level: note that electrons can flow easily from a pellet to the electrode it passes through, but not vice versa, as the pellet acts as a discharge point source while the treated electrode surface is smooth.

Focussing to keep the pellets centered during acceleration is provided by electric or magnetic fields, e.g. quadrupole magnets as used in particle accelerators.

Pellets are strength-tested by charging them to slightly above operational voltage before firing. In-tube pellet failure is therefore unlikely. Any failure which does occur has the potential to become contagious. However worst-case energy release in a tube is 2 MJ. The tube can be wrapped in a Kevlar blanket so that the MOSFET switches and other tubes are not damaged.

Chicane wiggles can be incorporated at multiple points in the system: slight bends with lateral electric fields which divert pellets of exactly the correct charge/mass ratio into the next section, but allow any other material to fly on into open ended 'dump tubes' in which the plasma from their impact is safely contained.

The overall electrical efficiency of the accelerator is $\sim 70\%$. Pellet trains of kinetic energy 8 MJ are provided at rate 10 Hz, so total accelerator consumption is ~ 120 MW.

Unlike lasers, the repeat firing rate and service life of the accelerator are essentially unlimited, and its maximum power delivery rate is not constrained by laser-plasma interactions. Its overall cost, calculated in section 2.7, is vastly less than that of equivalent lasers.

2.4 STANDOFF PIPE

90,000 pellets emerge from each accelerator tube over a period of 0.64 ms, in a train of initial length 450 m. All pellets reach a common point 2.25 km downstream at the same instant, after passing along a vacuum pipe (or separate near-parallel converging pipes) of this length.

Containing a relatively soft vacuum by particle accelerator standards, the standoff pipe(s) need not be housed in a building but can be mounted on pylons or stilts. The pipe(s) are given a larger internal radius than the maximum pellet deviation from the beamline, so that lateral displacements due to wind etc. of several centimetres can be tolerated, and also so that vacuum can be maintained by pumping from a small number of points along their length. The vacuum pumps are mounted in Portakabin-size units stationed every 750m, which also contain the course correction systems.

The pellets must be steered to high precision, a few microns, to ensure that none collide before reaching the hohlraum with potentially disruptive effects, and that the hohlraum membrane is heated evenly. To this end their individual trajectories are measured and corrected at several successive points during flight.

Trajectory measurement can be made as follows: the passage of each pellet produces an induced voltage/current in small wire loops set closely around each beamline. Each beamline constitutes a current ranging from 55 mA @ 126 MHz to 4 mA @ 462 MHz as seen over time at the various course correction stations: the voltage induced by each pellet is amply large enough to be measured with high precision at a point closely adjacent to the flow. The readings from three or more loops allow the position of each pellet to be calculated.

(Even more accurate pellet position measurement could be done if required. With picosecond pulse lasers providing exposure control, cameras with cheap CCD or CMOS sensors and microscope-style lens turrets can photograph passing pellets to $\sim 1\mu\text{m}$ precision. With some on-chip preprocessing, a slightly more sophisticated version of pixel binning,

to reduce the data volume to be transferred, each camera can report the position of hundreds of pellets per pulse.)

After measurement, individual trajectories are tweaked as required in the vertical and horizontal directions, and optionally also in speed. Lateral steering could be done using either electric or magnetic fields. At relativistic speeds in a fundamental particle accelerator, magnetic fields are more effective. However at 700 km/sec, the lateral force from a 1 Tesla magnetic field is equivalent to only a 700 V/mm electric field, whereas a switchable electric field of at least 40 kV/mm across the beamline can easily be provided. Electric fields are therefore used. To apply independent corrections to each pellet, electrode length should be about half the pellet separation, which reduces from 5 mm at accelerator exit to 1.7 mm at the final correction station.

A 40 kV/mm lateral field would deflect the fastest fully charged pellet 0.33 microradians per millimetre of electrode length. In practice, to minimize inter-pellet interaction in the beamline, pellet charge is reduced by a factor 20 immediately after the first course correction on accelerator exit, a further factor 2 immediately after the second course correction, and to zero after the final course correction, eliminating mutual repulsion at convergence. Discharge is performed by electron guns supplying 220 mA current in total.

Reducing the pellet charge by factor n increases the total electrode length needed for a given steering adjustment proportionately. However, many consecutive independently switchable electrodes can be provided, so there is no practical limit to the size of course correction that can be applied. The total number of steering electrodes and associated solid state switches needed is small compared to the accelerator.

The beamline is kept as narrow as possible until the final course correction station. At that point, individual pellets are intentionally deflected up to several microradians from the beamline, so that they will arrive at the hohlraum membrane laterally displaced up to several millimetres from its central point, achieving uniform coverage of the membrane in whatever

precise pattern desired. About one metre length of consecutive electrodes are required.

The rate of pellet flow past a given point peaks at 462 MHz per beamline at the final course correction station. Solid state power switches capable of > 20 GHz operation are commercially available, as are 12-bit ADCs capable of sampling rates up to 3.6 GHz^[13], so this can easily be handled.

Pellet steering is sufficiently precise that unintended premature collisions between pellets do not occur. The most concentrated mass flow rate required is at the trailing edge of the second wave entering the hohlraum, which must supply $\sim 4 \times 10^{15}$ W/cm² kinetic energy. An average density of ~ 0.25 g/cm³ is required, implying pellets which in solid form are separated by about one pellet diameter clearance if made of Weldalite, or two pellet diameters if maraging steel.

(The first 'preheat' wave of pellets may be intentionally made to collide with one another just before hitting the hohlraum membrane, turning them to a relatively uniform vapour or plasma before impact. The motivation is to avoid pellets impacting the membrane while still solid, which could seed Rayleigh-Taylor instabilities. All subsequent pellets will be vaporised before impact anyway, by heat radiated backward from the collision plasma.)

2.5 REACTION CHAMBER

A particular advantage of the system is that a vacuum chamber is not required for the fusion. By using a sacrificial projectile to protect the pellets during the final part of their journey, the detonation can be made to take place in a void surrounded by a lithium waterfall which should provide 50-100 cm thickness of liquid lithium: 1-2m waterfall thickness if the lithium droplets are 50% space-filling.^[14]

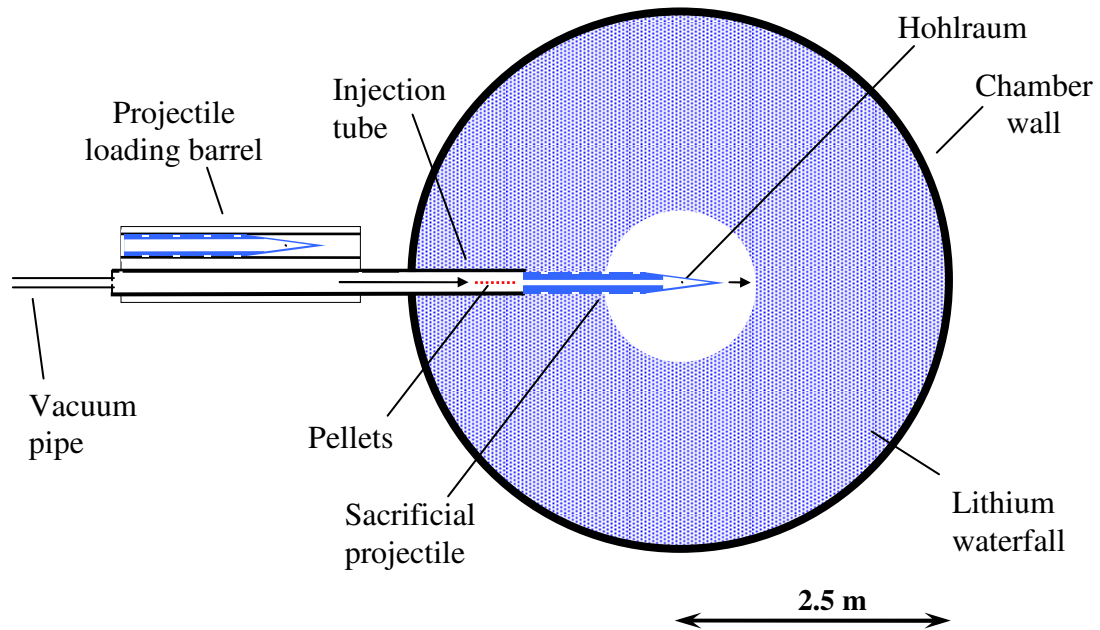
80% of the fusion energy released goes to heat the liquid lithium by neutron interaction. The remaining 20% is in the form of energetic α -particles. This vaporises the hohlraum. However because this constitutes a small mass, $\sim 1\text{g}$, although the energy absorbed is 40 MJ the associated momentum pulse is only $\sim 100\text{ kg}\cdot\text{m/s}$. This high-speed plasma loses almost all its kinetic energy as it strikes the droplets of the lithium waterfall, and while the associated outward momentum is not lost, it reaches the chamber wall as a relatively lengthy pulse of modest overpressure rather than an intense shock wave.

The lithium is circulated through a heat exchanger by electromagnetic pumping. Lithium has high boiling point and heat capacity, 1347°C and 3.85 J/gK , with density 0.5 g/cc : in theory a flow of as little as $2\text{ m}^3/\text{sec}$ could extract enough heat to generate 1 GW electricity. In practice a flow rate several times larger will be used, both for reasons of thermodynamic efficiency, and to provide the 'waterfall' which protects the chamber walls. 1 metre net lithium thickness gives a stainless steel chamber an indefinite working life.^[14]

Almost all neutrons produced are absorbed by the lithium to breed tritium. Initial high energy neutrons from the DT reaction can be absorbed by ^7Li to produce both a tritium atom and a lower energy neutron, which can breed a further tritium atom from ^6Li . Natural lithium comprises a mixture of these isotopes, 7.5% ^6Li to 92.5% ^7Li : this ratio can easily be altered by fractional distillation. Thus it is straightforward to fine-tune the system so that exactly 100% of the tritium required for continued operation is produced.

FIGURE 4 Reaction chamber

(not to scale: actual pellet number will be thousands, each 0.04mm diameter)



The chamber is shown in Figure 4, as seen from above in cross-section: the lithium flows vertically down into the page, to collect in a sump. The sacrificial projectile comprises a hollow tube open at the rear, with the hohlraum containing the fuel capsule fixed at the forward end. The projectile is fired into the reaction chamber at ~ 100 m/s. The pellets subsequently travel through the good vacuum preserved in the projectile interior to strike the hohlraum foil.

Trailing pellets can be made to strike the interior walls of the projectile immediately after the main cloud passes, evaporating lithium to provide a complete seal against escaping neutrons and radiation on detonation.

The outer walls of the projectile can be notched as shown to create toroidal cavities which act as a cascade of cold traps. Traces of lithium vapour escaping past the projectile could compromise the good vacuum behind and within it: this arrangement ensures that none does so. The rotating barrel used to insert projectiles acts as a barrier between the chamber and the standoff pipe at other times: additional doors, cold traps for metal vapor and electrostatic traps for light gas atoms can be provided.

The injection tube helps the projectile pass through the lithium waterfall without losing too much speed. While the chamber itself has indefinite life, the injection tube is inexpensive and can be replaced at regular intervals. Nevertheless it is well protected at the moment of detonation: neutrons and blast wave must pass through a long slant length of projectile wall before reaching any part of it.

The sacrificial projectiles need to be made cheaply and continuously on-site. They can be made by tapping the circulating molten lithium and pouring it into moulds. Tritium and unburned deuterium is also recovered from the molten lithium as it circulates, a simple separation as there is no other hydrogen present.

Overall size of the chamber is partly determined by the gap size required between the central point and the inner side of the lithium waterfall. At the inner side of the waterfall, each centimetre thickness of lithium intercepts $\sim 1.5\%$ of the fusion energy flux.^[14, interpolated from Figure 6] It is desirable that this is not sufficient to boil the lithium: allowable energy deposition can be up to 1.5 kJ/cc if the coolest lithium emerging from the heat exchanger is sprayed at the inner side of the waterfall. For 200 MJ thermal energy fusion detonations in the baseline system, this implies an inner waterfall surface area of 2,000 cm², inner radius 13 cm. In theory, chamber diameter could be as little as 2 metres. However, centrally released alpha-particle energy is sufficient to vaporise some 10 kg of lithium per pulse from cold, much more if the inner lithium is already raised to near boiling point by neutron energy. While such evaporated vapour quickly recondenses on other droplets, a more reasonable minimum chamber diameter is 5 m, providing 1m net thickness of liquid lithium at 50% volume fill plus a 50 cm inner waterfall radius. This will give a stainless steel containment chamber an indefinite working life.^[14]

2.6 OUTPUT CYCLE AND EFFICIENCY

Thermal energy available after capsule detonation is 200 MJ from fusion, plus 40 MJ from fission in the lithium blanket surrounding the reaction, plus the 8 MJ kinetic energy originally input = 248 MJ. This generates 112 MJ of electricity @ 45% efficiency, of which 12 MJ is required to generate the next pellet pulse. Net electricity output is 100 MJ, as summarised in Table 5. Ten detonations per second can drive a 1-GW power station.

TABLE 5 Energy per detonation

Thermal input	MJ
Kinetic energy of pellets	8
Fusion energy	200
Fission in lithium waterfall	40
Total	248
Electricity generating efficiency	x 0.45
Gross electric output	112
Returned to accelerator	12
Net output	100

Future generation lasers of suitable type are unlikely to be more than 18% efficient^[3], so overall efficiency of the pellet system is better than lasers, despite the higher ratio of kinetic energy supplied to X-ray energy received by the capsule.

2.7 SIZE AND COST

Electrical engineering

The largest single cost element of the accelerator is the RF power MOSFETs: total approximately \$30 million, as calculated in section 2.3.

Since duty cycle is low, ~2%, time-averaged power is only about 1/3 of the maximum the chip can provide: power supply and cooling cost will be relatively modest.

Volumetric cost of raw materials for the accelerator tube itself are ~\$80/litre for Rexolite insulator, ~\$60/litre for virgin grade Teflon, ~60/litre for copper. Volume required is ~1,000 litres per tube, so total cost is less than \$0.5 million.

To allow for power supply, installation, control systems and auxiliary equipment such as the feeder system and trajectory adjustment stations, total electrical system cost is nevertheless put at three times the MOSFET cost: \$90 million.

Civil Engineering

A 1.6 km long building is required to house the accelerator and its feeder, providing an environment of dry air at constant temperature. Single-storey industrial buildings typically cost ~\$1,500/m² footprint^[15]. On this basis a building consisting of a 4m wide corridor would cost \$6,000/m. However the building must run straight and level for the length of a mile. Ground preparation cost may therefore be higher than normal. A double-track railroad on cheap land without geophysical complications costs^[16] ~\$5,000/m. Total cost of the accelerator building, including foundations and construction, is therefore put at \$10,000/m = \$16 million.

Standoff pipe cost is assumed similar to a 69kV single-circuit overhead transmission line^[17]: 2.25 km @ \$300/m = \$0.7 million.

Total accelerator system cost is therefore put at **\$110 million**.

The capital cost per GW of a conventional power station is around^[18]:

\$1.5 billion – coal-burning

\$1.5 billion – conventional hydroelectric

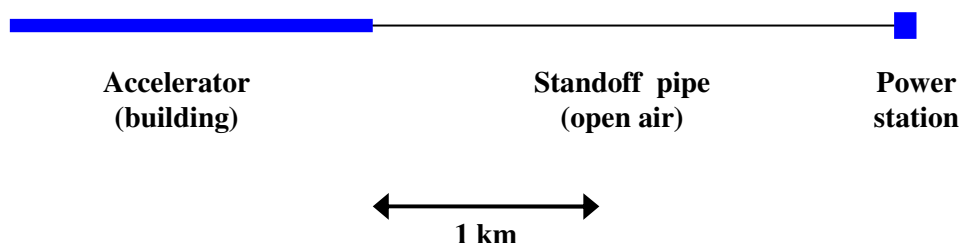
\$0.5 billion – gas turbine

The capital cost of a 1-GW fusion station will be less than 10% greater than an equivalent coal-fired plant generating electricity from steam. The additional element allowed is the accelerator cost only: the lithium chamber and its associated recycling equipment are assumed to replace a conventional furnace and coal handling equipment of comparable or greater cost.

Fuel cost will be negligible, compared to ~\$250 million/annum for a 1 GW coal-fired plant. The fusion system will recoup its cost within one year.

Existing coal-fired plants, which already have steam turbines, cooling towers and generators, can be retrofitted for fusion. Even if constraints of topology or surrounding urban development make it necessary for the entire length of the accelerator and standoff pipe to be housed in tunnels dug for the purpose, the additional cost of tunnelling will be ~\$36,000/m for the accelerator, ~\$20,000/metre for the standoff pipe, total \$100 million, roughly doubling the cost of the accelerator system.

FIGURE 5 Overall system length



2. DEVELOPMENT AND OPTMIZATION

Guided impact fusion will be a highly attractive option for all large scale energy generation, competitive on commercial grounds alone.

The necessary expertise for fast-track development, scientists and engineers with experience of building large particle accelerators, is already available.

All components of the accelerator and guidance system are COTS-available.

There is therefore a strong case for proceeding immediately on a commercial basis, bypassing the glacially slow pace of academic research and government-funded development.

A laboratory-scale version can prove all aspects of the accelerator concept. Given an accelerator, further optimisation can be done mainly in software, by making changes to the pellet trajectories.

The most attractive aspect of guided impact fusion is its scalability and flexibility.

3.1 REDUCING THE IGNITION PULSE ENERGY REQUIRED

The 8 MJ kinetic input assumed for the baseline system is almost certainly pessimistic, for the following reasons:

- Increasing the pellet speed is beneficial in two ways:

As the total pellet mass becomes smaller relative to the mass of the stationary membrane, less energy is wasted in the final linear kinetic energy of the collision plasma.

As the ratio of the energy input to the total collision plasma mass becomes higher, less energy is wasted in the final internal heat of the collision plasma.

This allows a substantially higher overall efficiency.

- Research (theoretical and experimental) for both fast ignition and z-pinch fusion shows that implosion of a fully spherical fuel capsule may not be necessary: imploding a hemisphere backed by a 'glide plate' of dense metal, or indeed a cone of almost any apex angle, may work almost as well. If a hemisphere or cone whose curved base faces the oncoming pellets is used, coupling between the collision plasma and the capsule is excellent: very little X-ray energy is wasted.
- The mass distribution of the pellet cloud can be tailored in software alone, with the trajectory of each of the thousands of pellets set independently. It will be possible to produce a pulse shape far more precisely tailored to the optimum than is possible with lasers.

It may well be possible to increase the ratio of capsule-received energy to hohlraum-received energy from the 12.5% assumed for the Baseline Design to something nearer the 25-35% aspiration for the LIFE and NIF laser-driven designs.

3.2 INCREASING THE IGNITION PULSE ENERGY AVAILABLE

Past experience of fusion development suggests that it will be wise to be able to provide much more than the theoretically calculated input energy if necessary. Greater energy input and output per pulse is anyway beneficial as it allows fewer fuel capsules and hohlraums to be used per GJ of output energy. Fuel capsules and hohlraums also become cheaper to manufacture, due to reduced tolerance requirements.

The cost of the accelerator RF MOSFETs increases linearly with the total energy provided in the input pulse. However the cost of other elements increases much more slowly. For example to provide 8 times the input energy using the same number of pellets at the same delivery speed, pellet diameter doubles. This halves the charge/mass ratio possible for the pellets, only doubling the civil engineering cost element of the accelerator.

To maintain a favourable energy output ratio, the thermal energy obtained per detonation would also need to increase eightfold, to ~ 2 GJ. However

this does not increase the cost of the containment chamber proportionately. The thickness of lithium waterfall needed is almost constant regardless of detonation size. It is only the inner radius of the waterfall that needs to increase, to avoid neutron energy alone being sufficient to vaporise the inner layer of lithium. If detonation energy increases 8 times, the inner area of the waterfall should also increase by 8, hence the inner radius by a factor of ~ 3 , to 1.5 m. Overall chamber diameter becomes 7 m: total chamber volume is less than triple that of the baseline system.

It will be therefore be possible to increase the input pulse power by a factor of 10 or more while keeping capital cost acceptable.

There is an enormous margin, two orders of magnitude, between the maximum energy that could be delivered by the accelerator if necessary, and the minimum calculated to be required. In stark contrast to every other fusion system proposed to date, technical risk is close to zero.

APPENDIX: ELECTRIC FORCES WITHIN AND BETWEEN PELLETS

Maximum charge which can be placed on a pellet is limited by burst-apart due to self-repulsion. As the pellet is a sphere, charge will distribute itself evenly over the surface. The force calculation is then mathematically identical to the well known case of the self-gravity of a thin spherical shell. A point mass m at a distance R from the centre of a spherical shell of mass M experiences a gravitational pull of GmM/R^2 in the space outside the shell, and zero everywhere inside it. An average particle of the shell itself thus experiences $GmM/2R^2$. The mass per unit area is $M/4\pi R^2$, giving an inward surface pressure of $GM^2/8\pi R^4$.

The corresponding outward pressure on a spherical shell carrying charge Q is $kQ^2/8\pi R^4$, where $k = 1/4\pi\epsilon_0$. This must not exceed the safely usable strength σ of the material, so maximum charge permissible is $5.3 \times 10^{-5} R^2 \sqrt{\sigma}$. The mass of the sphere is $(4/3)\pi R^3 \rho$, so the maximum charge/mass ratio is:

$$Q/M = \frac{1.26 \times 10^{-5} \sqrt{\sigma}}{R\rho}$$

where σ is the usable tensile strength of the material after allowing a suitable safety factor.

The maximum charge which can be held is also limited by field effect evaporation (assuming a positively charged sphere: field effect evaporation typically requires a much higher field than field electron emission). Capacitance of the pellet is $4\pi\epsilon_0 R$, potential $V = Q/4\pi\epsilon_0 R$, so surface field strength is $Q/4\pi\epsilon_0 R^2$.

As regards inter-pellet interactions, the repulsion between two point charges q at separation r is kq^2/r^2 where $k \approx 9 \times 10^9$. At distance ~ 5 mm (the separation with which they leave the accelerator) the force between two pellets each carrying charge 0.44 nC is 70 μ N, which accelerates each at 8×10^5 m/s². Theoretically, the opposing forces from nearest neighbours ahead and behind should cancel. However there is a stability problem in that a pellet displaced slightly from the nominal beamline will experience a lateral force proportional to the displacement.

Within the accelerator, this stability problem does not arise, as the electrode-induced acceleration is $\sim 10^8 \text{m/s}^2$, two orders of magnitude greater than the inter-pellet repulsion. However once in the standoff pipe, any small lateral displacement will tend to grow exponentially. At 5mm linear separation, a pellet displaced $1\mu\text{m}$ from the beamline will experience lateral force 28 nN, accelerating it at 300m/s^2 : the time constant for the lateral displacement to double $\tau \sim 60 \mu\text{s}$, during which the pellet travels a linear distance ~ 40 metres.

τ scales as $q^{-1} \cdot d^{1.5}$ where q is pellet charge and d is pellet separation. Although the unwanted lateral acceleration can be calculated from the relative pellet position as seen by the monitoring cameras, hence allowed for in calculating the course adjustment required, it is desirable to keep τ no larger than the approximate time of flight between consecutive course correction stations, which is 1 ms. If pellet charge is reduced by factor 20 immediately after the first course correction on accelerator exit, a further factor 2 following the second course correction, and to zero after the final course correction, this is achieved.

REFERENCES

1. A1.5 Fusion Performance, P. Amendt, LLNL-TR-477871 (2011)
<http://e-reports-ext.llnl.gov/pdf/482669.pdf>
2. The Physics Of Inertial Fusion, S. Atzeni & J. Meyer-Ter-Vehn
OUP (2004)
3. Compact, Efficient Laser Systems required for Laser Inertial Fusion Energy;
to appear in Fusion Sci. Technol. (2011)
<http://yag1.kaist.ac.kr/hjkong/>
4. Opacity Calculations Of Low Z Plasmas for ICF, J Rubian et al (2008)
35th EPS Conference on Plasma Physics, ECA Vol.32D, P-2.147
http://epsppd.epfl.ch/Hersonissos/pdf/P2_147.pdf
5. Hypervelocity microparticle characterization, G.C. Idzorek, Los Alamos (1996)
<http://www.osti.gov/bridge/servlets/purl/397131-QIEjdF/webviewable/397131.pdf>
6. The Nanoscale Strength of Ultra Nano Crystalline Diamond, N. Pugno (2005)
Rev.Adv.Mater.Sci. 10 (2005) 156-160
www.ipme.ru/e-journals/RAMS/no_21005/pugno.pdf
7. <http://www.matweb.com/search/datasheetText.aspx?bassnum=MA9WELD8>
8. Field-evaporation from first principles; C. Sanchez & A. Lozovoi
<http://citeseerx.ist.psu.edu/viewdoc/download?doi=10.1.1.62.9026&rep=rep1&type=pdf>
9. The Dielectric Wall Accelerator, G. Caporaso, Y. Chen & S. Sampayan
(2009) LLNL-JRNL-416544
<http://e-reports-ext.llnl.gov/pdf/377059.pdf>
10. Investigations Of DC Breakdown Fields, T. Ramsvik et al. (2006)
Proc. EPAC 2006, Edinburgh, Scotland
<http://accelconf.web.cern.ch/AccelConf/e06/PAPERS/MOPLS095.PDF>
11. http://www.ixysrf.com/pdf/switch_mode/IXZ210N50L.pdf
12. <http://uk.farnell.com/ixys-rf/ixz2210n50l/mosfet-n-rf-754/dp/1347729?Ntt=ixz2210n50l>
13. http://www.national.com/en/adc/ultra_high_speed_adc.html
14. Reactor Concepts for Laser Fusion, W Meier & J Maniscalco
<http://www.osti.gov/bridge/servlets/purl/5232953-TPTXcg/5232953.pdf>
15. Building Costs In Illinois
<http://www.ildceo.net/NR/rdonlyres/2E961958-4860-4526-806B-2705C5F42339/0/BuildingCosts.pdf>
16. Calculating Rail Construction Costs In Light Of The Eddington Report
<http://melbpt.wordpress.com/2008/04/26/calculating-rail-line-construction-costs-in-light-of-the-eddington-report/>
17. Underground Electric Transmission Lines
<http://psc.wi.gov/thelibrary/publications/electric/electric11.pdf>
18. Estimated Capital Cost of Power Generating Plant Technologies
<http://www.jcmiras.net/surge/p130.htm>